- This is the accepted manuscript version of the article. It has been revised following peer-review by the ***Journal of Environmental Management.***

- It is recommended that readers cite the original article as follows:

  Yu, Q., Rennie, C. D., Slaney, J. M., & Parsapour-Moghaddam, P. (2022). Impact evaluation of instream bar management using morphodynamic modeling. Journal of Environmental Management, 318, 115564. https://doi.org/10.1016/j.jenvman.2022.115564

- Both versions contain the same content but differ in formatting.

Impact evaluation of instream bar management using morphodynamic modelling

Qingcheng Yu[1], Colin D. Rennie[1], Jonathan M. Slaney[2] & Parna Parsapour-Moghaddam[3]

[1] Department of Civil Engineering, University of Ottawa, Ottawa, Canada, K1N 6N5

[2] River Engineering Group, City of Calgary, Calgary, Canada, T2P 2M5

[3] Environment and Climate Change Canada, Gatineau, Canada, J8X 4C6

Corresponding author: Qingcheng Yu (qyu101@uottawa.ca)

Highlights

- Appropriate bar realignment can provide aquatic habitat and river recreation.
- Bar removal performs the best in terms of flood mitigation compared to other plans.
- Manipulation on instream bars has little morphological impact to downstream reach.
- Creating a less obstructed channel is the fundamental strategy in flood mitigation.

Abstract

The Bow River's 2013 flood was the costliest natural disaster in the City of Calgary's history. Flood-induced bar growth and subsequent riparian vegetation colonization at many locations has constricted the river channel, which increases flood risk. Although bar removal has been widely employed as a flood mitigation strategy, its effectiveness and associated impacts are still uncertain. This study employs Delft3D to develop a two-dimensional (2D) morphodynamic model in order to evaluate the impacts of a conventional plan of bar removal and a novel plan of bar realignment in terms of flood mitigation, aquatic habitat protection and river recreation realization. A hydrodynamic model was firstly developed and calibrated using post-flood spatially distributed velocimetry data. A morphodynamic model was then developed and validated using post-flood bed elevation survey data. Then, the future channel response and flood peak levels using different bar management plans were modelled and compared. Results show that appropriate bar realignment can protect aquatic habitat and provide river recreation opportunities while bar removal performs the better in terms of lowering the future flood peak level. The findings indicate that manipulation on instream bars has little morphological impact to downstream reach and creating a less obstructed channel is the fundamental strategy in flood mitigation.

Keywords

Morphodynamic modeling; gravel bar; bar removal; bar realignment; flood; aquatic habitat

1 Introduction

In river morphology, bars are elevated sandy or gravelly bedforms in river channels that are usually exposed at normal water level while submerged at high water level (i.e. floods). Bars are one of the most common geophysical features in fluvial systems. Based on the different regions of bar formation, bars can be classified as mid-channel bars, bank-attached bars, and river mouth bars (Church 1992), and based on sediment size, as gravel bars or sand bars. Fundamentally, bars form at the places where sediment supply rate is higher than the sediment transport capacity of the flow.

In gravel-bed rivers, bars are likely to be created and grow during floods due to the excessive amount of bedload carried by floodwater (Mat Salleh & Ariffin, 2013; Parsapour-Moghaddam et al., 2019b; Wintenberger et al., 2015). After floods, those flood-induced gravel bars become stabilized due to the drop of flow velocity. Subsequent riparian vegetation colonization on the exposed bar surface can further stabilize the bars (Rood et al., 2019). Gravel bar formation is part of a rivers natural migration process and provides important habitat for benthic invertebrates, waterbirds, and fish species such as salmon and trout (Church et al.,2000; Kondolf & Wolman, 1993; Miller et al., 1983; Rempel et al., 2012; Zeng et al., 2015). However, when bars form on managed rivers, they may block the channel, cause navigation difficulties, and pose future flood risks to riverine societies (Petit et al., 1996). The flood risk can increase when riparian vegetation colonization on the bar surface induces additional resistance to the flow, thus cause sediment aggregation around the bar during the next flood event (Church et al., 2001; Rood et al., 2019), resulting in a "vicious circle" of bar and vegetation growth.

Since the late 19th century, instream gravel extraction and bar removal has been widely applied as a cost-effective way to supply aggregate to the construction industry as well as mitigate flood risks and ensure channel navigation (Church et al., 2001; Kondolf, 1997; Sear & Archer, 1998; Wishart et al., 2008). However, gravel removal may generate a deficit in the active fluvial sediment balance, such that the flow becomes sediment-starved (Kondolf, 1997), resulting in consequences such as channel incision, bed coarsening, undermining of structures, and destruction of aquatic habitat (e.g. Brown et al., 1998; Collins & Dunne, 1989, 1990; Pauley et al., 1989; Petit et al., 1996; Sear & Archer, 1998; Surian, 1999; Kori & Mathada, 2012). A field study done by Wishart et al. (2008) suggested that removing sediment from vegetated bars (indicative of long-term storage) is considered to be less likely to generate a deficit in the active fluvial sediment balance and possibly a safe method to mitigate flood risk, yet not proven.

Bar realignment could be an alternative bar management plan as opposed to bar removal. Bar realignment refers to the modification of the layout of instream bars within the channel without significantly changing the total volume of bars. Theoretically, bar realignment could have the following advantages compared with bar removal:

- Bar realignment can preserve the volume of instream bars, which brings no disturbance to the reach-scale sediment budget. Thus, it is reasonable to speculate that appropriate bar realignment is less likely to cause downstream incision compared to bar removal;
- By realigning instream bars, the local flow field and sediment transport patterns will be altered. This alteration could result in a favorable condition in terms of inhibiting future bar growth and channel stabilization, and possibly, lowering the

future flood level;

- Appropriate bar realignment has the potential to increase the diversity of river flow & channel bed conditions. This diversity can potentially provide an ideal condition for new habitat as well as the realization of river recreation (e.g. swimming, surfing, kayaking, etc.);

However, to the best of the authors' knowledge, the practice of bar realignment has not been addressed in the literature and is therefore unproven. In summary, there are still research gaps and also opportunities in the evaluation of instream gravel management in terms of flood mitigation, morphology, aquatic/riparian habitat, and recreation.

Morphodynamic modelling could be an efficient tool to study those impacts of instream gravel management. Once properly calibrated and validated, morphodynamic modelling has the potential to predict future consequences of different gravel management plans under different flow conditions. Nonetheless, the morphodynamic studies on gravel management are extremely scarce (e.g. Li et al., 2008; Parsapour-Moghaddam et al., 2019b; Yuill et al., 2016) and preliminary: first, those models are not properly calibrated/validated due to the lack of reliable field data. In addition, those models have very limited ability to evaluate downstream channel response due to gravel management. In summary, the powerful tool of morphodynamic modelling hasn't been fully exploited in the field of instream gravel management.

The objective of this study is to evaluate the performance of three instream gravel bar management plans in Bow River, Calgary in terms of morphological impacts, future flood risks, aquatic habitat protection, and possible river recreation use through morphodynamic modelling.

The major novelty of this study is that we propose a new instream bar management strategy of bar realignment and demonstrate its promising applications in river engineering. This study demonstrates that manipulations on long-term vegetated gravel bars have little morphological impacts to downstream areas, which fills a research gap in instream bar management. This study also implies that a more efficient strategy in fluvial flood mitigation is to create a uniform, less obstructed river bed, compared to river bed widening or lowering.

This study was carried out using the Delft3D platform. A hydrodynamic model was first developed and calibrated against existing velocimetry data. Then, a morphodynamic model was developed to simulate a large flood event and validated against the post-flood bathymetric survey data. Afterwards, three bar management plans: "do nothing", "bar removal", and "bar realignment" were implemented respectively by altering the river bed DEM (Digital Elevation Model). Following that, future performances of those plans were evaluated numerically and compared in terms of flood peak levels as well as morphological impacts.

2. Study area and data

The Bow River, located in southern Alberta, Canada, originates from Canadian Rocky Mountains and ends at the confluence with the Oldman River (Figure 1a & 1b). It has a length of approximately 645 km. It flows through three geographic regions: the mountains, the foothills, and the prairies (Veiga et al., 2015). The reach that passes

through the City of Calgary (will be noted as "the Calgary reach" hereafter) is situated at the geological transition region between foothills and prairies. According to the "conveyor belt" model raised by Kondolf (1994), the Calgary reach is the "zone of transport", which is characterized by gravel-sized bed sediment, channel meandering, and distinct instream bar formation. Several upstream reservoirs have cut off gravel transport, resulting in some surface armoring in the Calgary reach.

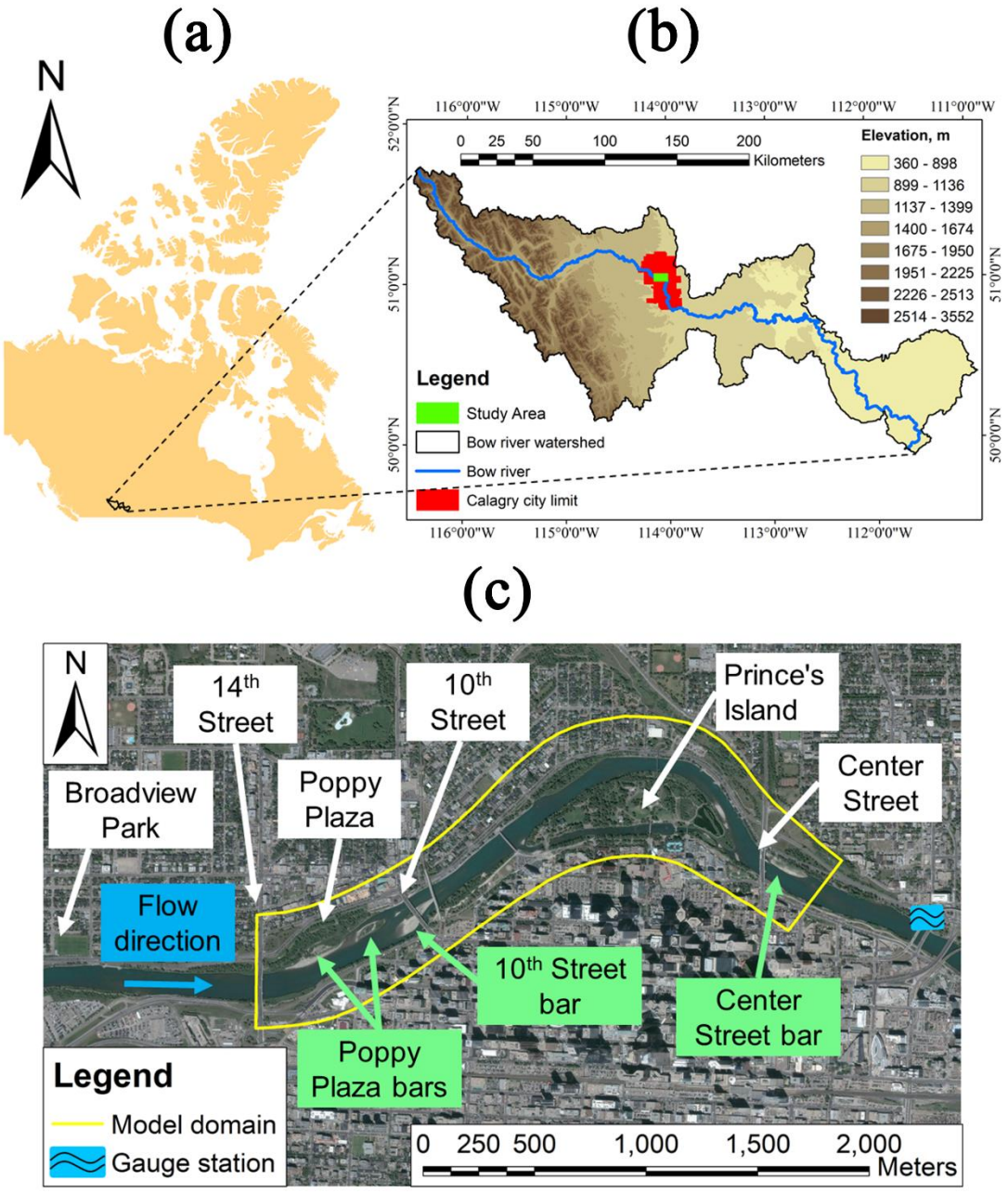

Figure 1. (a) The location of Bow River watershed in Canada. (b) The topography (courtesy of Dr. Atakan Erdem, University of Calgary) along the Bow River flow path (the blue line) and the location of the study area (the green area). (c) The model domain (the yellow polygon) and important landmarks. Background satellite image was taken in the year 2021, © Maxmar technologies, Google Image.

In late June 2013, with continuous heavy rainfall and rapidly melting alpine snow, the Bow River witnessed the highest flow of the century-long records (Pomeroy et al.,

2016). The flood inundated the downtown Central Business District (CBD) of Calgary, and resulted in the evacuation of 26 communities in Calgary and a total cost of $5 billion across southern Alberta, which makes the 2013 flood one of costliest flood events in Canada's history (Government of Alberta, 2014). The 2013 flood also produced up to 100 m of bank erosion in several locations of the Bow river as well as creation or expansion of extensive, barren, gravel bars and islands (Rood et al., 2019; Slaney et al., 2019). By the year of 2021, those gravel bars have been mostly vegetated, especially the largest ones that are close to the downtown CBD of Calgary: Poppy Plaza bars and 10th St. Bars (Figure 1c). Those bars might pose a flood risk to the city, thus, three alternate options have been considered for their management:

① **"Bar removal".** Bars will be fully removed in order to reduce future flood risks;

② **"Do nothing".** Bars will stay in the channel in order to avoid any possible consequences brought by human intervention;

③ **"Bar realignment".** Bars will be realigned to new sites without changing the total volume of instream bars significantly in order to fulfill multiple needs: reduce future flood risks, restore/create aquatic habitat, minimize downstream morphological impacts, and create a river surf wave park (Surf Anywhere, 2020) near the 10th St. bar.

The model domain starts from the 14 St. SW Bridge to the Center Street bar in the Bow River (See Figure 1c). The total length of this reach is about 3.3 km. The average width of this reach is about 85 m. The reasons and advantages of choosing this reach as the model domain are:

- **Distinct bar growth.** During the 2013 flood, this reach witnessed distinct bar formation and growth (See Figure 2), which provides the basis of model validation and implementation of different bar management plans;

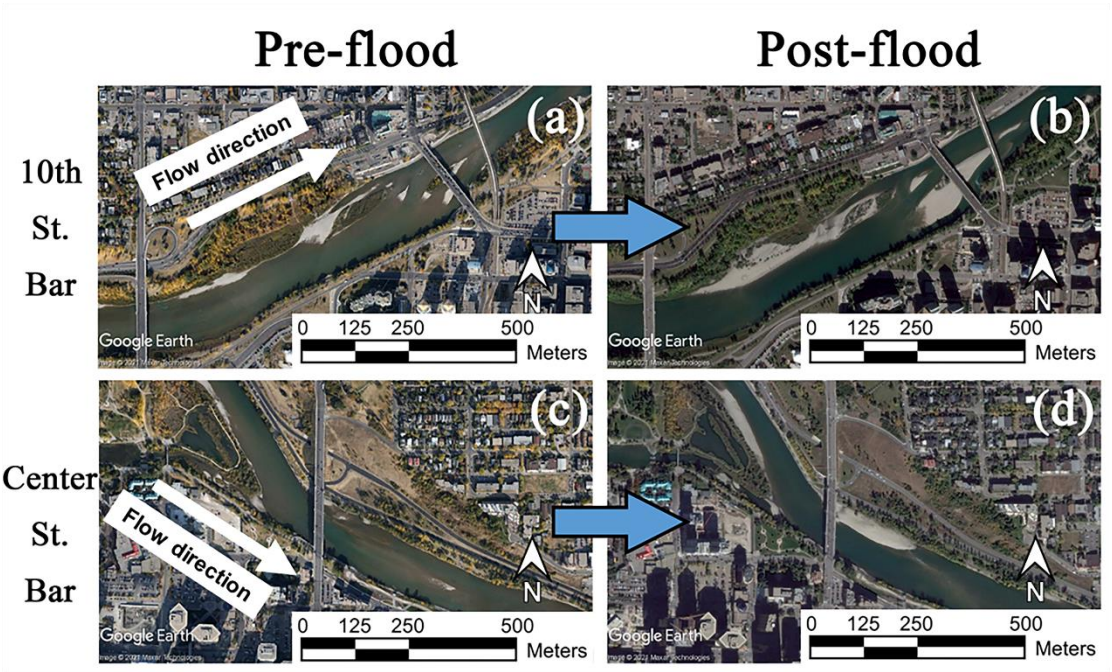

Figure 2. Aerial photographs of the Bow River before (Sep, 2012; $Q \approx 70\ m^3/s$; sub-figure "a" & "c") and after (Sep, 2014; $Q \approx 95\ m^3/s$; sub-figure "b" & "d") the 2013 flood for the 10th St. bar (sub-figure "a" & "b") and the Center St. bar (sub-figure "c" & "d"). Image © Maxmar technologies, Google Image.

- **Complete dataset support.** Abundant survey data and gauged data are available (See Table 1) in this reach, which provide essential supports to build and test the numerical model.

Table 1.

Summary of the available dataset in the model domain.

Data type		Date	Coverage	Spatial Resolution	Source
Survey data	Bed elevation[#1]	2010/9/9	Whole model domain	River bed: 2.5 m x 40 m	Golder Associates (2011)
		2013/10/28		Dry land: 0.2 m x 0.2 m	Golder Associates (2015)
	Velocimetry (ADCP)	2013/9/9	A portion[#2] of the model domain	0.5 m x 100 m	Golder Associates (2015)
	Bed sediment gradation	Year 1986	N.A.	Surface layer	Northwest Hydraulic Consultants Ltd. (1986)
		Year 2016	10 St. Bridge & Center St. Bridge	Surface layer, Sub-surface layer	Klohn Crippen Berger (2016)
Gauged[#3] data	Discharge	1911-2019, Daily	N.A.	N.A.	Water Survey of Canada (2013)
	Water level	2012-2019, Daily			
	Bedload rate	1972-1978, Daily			

[#1] Data were collected using ADCP (Acoustic Doppler Current Profiler), land-based RTK (Real-Time Kinematic) GPS, and LiDAR (Light Detection and Ranging).

[#2] See Figure 3 for more details of the velocimetry survey coverage.

[#3] See Figure 1c for the location of the hydrometric gauge station.

2. Methodology

This study utilized Delft3D-FLOW to simulate the flow, sediment transport, and morphological updating process. In the hydrodynamic aspects, Delft3D-FLOW solves the Navier-Stokes equations for an incompressible fluid, under the shallow water and the Boussinesq assumptions (Deltares, 2020). In the morphodynamic aspects, Delft3D-FLOW solves the advection-diffusion (mass-balance) equation for suspended load transport and standard (e.g. Van Rijn, 1993) or user-defined formulations for bedload transport. The bed elevation is dynamically updated at each computational time-step by solving the Exner (1925) equation. Delft3D-FLOW has been widely used in several hydro-morphodynamic studies (e.g. Kasvi et al., 2015; Parsapour-Moghaddam et al., 2017, 2019a, 2019b; Williams et al., 2016; Yuill et al., 2016) and proved its powerful and reliable performance.

2.1 Hydrodynamic model

A 2-D hydrodynamic model was initially developed under a low-flow condition for which velocity data were collected following the 2013 flood, without considering the sediment transport or morphological updating process. The velocity data were used to calibrate important model variables such as background horizontal eddy viscosity (used to model 2D turbulence as well as dispersion) and Manning roughness (used to model boundary shear stress), as will be covered in the next section.

The model domain covers the river channel and a portion of floodplains (See Figure 1c) in order to accommodate overbank flow and any possible bank erosion. Grid size was determined by considering the tradeoff between the computational cost and the desired model details as well as considering the dimension of instream bridge piers at the 10 St. SW Bridge (width $\approx$ 6 m). Given all these considerations, the initial average grid size was set as 6.9 m. The maximum orthogonality and aspect ratio of the model grid are 0.009 and 1.44, respectively, which are both within the recommended range by Deltares (2020).

The post-flood bed elevation survey data (surveyed on Oct 28, 2013) were used as the bathymetry input. Bridge piers were implemented by using "dry cells" in the model domain. Gauged discharge of 103 m^3/s and water level of 41.27 m (referenced based on the mean sea level) were used as the model upstream and downstream boundary conditions, respectively. Steady-state flow was used in the hydrodynamic model due to the negligible variation of discharge and water level within a day. Trial runs showed that the equilibrium state could be reached in the real-event time of 3 hours, which was then set as the event duration of the hydrodynamic model. The time step was determined as 0.023 min, considering the requirement that the Courant number should be smaller than 1. The initial background horizontal eddy viscosity was set as 0.1 m^2/s, which was adopted from Parsapour-Moghaddam et al. (2019b). The initial Manning roughness was set as 0.03, based on the recommended roughness for gravel-bed (0.028-0.035) in Phillips & Tadayon (2006).

2.2 Calibration & sensitivity analysis

Figure 3 shows the post-flood velocimetry survey routes and velocity magnitude, which was collected on Sep 9th, 2013 using RTK-ADCP, and were post-processed using in-house Matlab codes (Rennie & Church 2010). Although the velocimetry survey only covered the first 1/3 portion of the model domain, the calibration parameters determined from the first 1/3 portion could be applied to the remaining 2/3 portion of the model domain as there is the little variation of channel surface and flow properties between those two portions.

Table 2 shows the scenarios of model calibration and sensitivity analysis and the associated statistical results by comparing the modelled and measured values. The background horizontal eddy viscosity, grid size, and Manning roughness are calibrated using the following approach: First, different values of background horizontal eddy viscosity were trialed while keeping the other two variables constant (E series). After the optimal value of eddy viscosity was determined, the same procedure was done for Manning roughness (M series), and then the grid size (G series). Modelled velocities were triangularly interpolated to the locations of velocimetry survey points before carrying out the statistical analysis in order to eliminate the errors induced by spatial deviation between measured and modelled velocity points. The following statistical parameters were used in the statistical analysis:

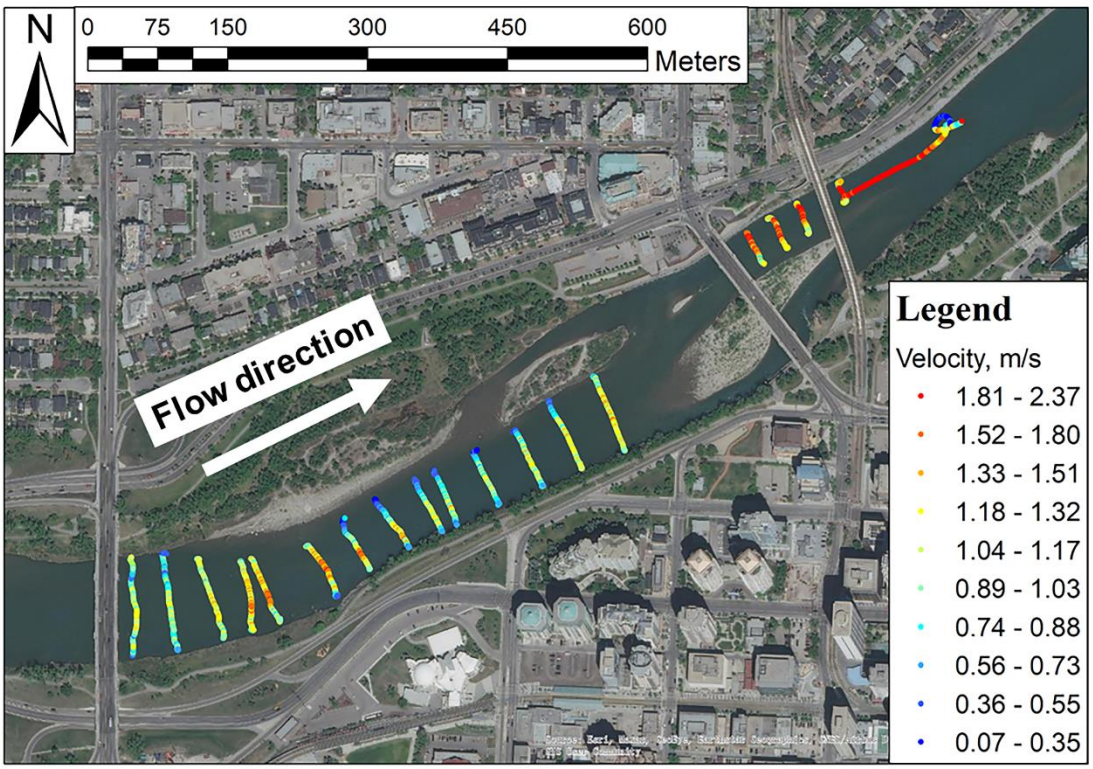

Figure 3. Post-flood (Date: 2013/9/9; $Q \approx 103\ m^3/s$) velocimetry survey routes and depth-averaged velocity magnitude. Background satellite image was taken in year 2021, © Maxmar technologies, Google Image.

$$R_{xy} = \frac{\sum_{i=1}^{n}(x_i - \bar{x})(y_i - \bar{y})}{\sqrt{\sum_{i=1}^{n}(x_i - \bar{x})^2} \cdot \sqrt{\sum_{i=1}^{n}(y_i - \bar{y})^2}} \quad (1)$$

$$MAE = \frac{\sum_{i=1}^{n}|x_i - y_i|}{n} \quad (2)$$

Table 2.

Model calibration and sensitivity analysis scenarios and corresponding statistical results.

Scenario	Setups			Statistical results	
	Grid size (m)	Eddy viscosity, m^2/s	Manning roughness	Correlation R	MAE, (m/s)
E 0.1	6.5	0.1	0.030	0.797	0.226
E 0.5		0.5		0.790	0.219
E 10		10.0		0.713	0.217
M 0.03	6.5	0.1	0.030	0.797	0.226
M 0.035			0.035	0.793	0.198
M 0.04			0.040	0.785	0.194
G1.1	1.1	0.1	0.035	0.804	0.190
G3.4	3.4			0.803	0.190
G6.5	6.5			0.793	0.198
G10.2	10.2			0.736	0.234

where R_{xy} is the Correlation R between two variables, x and y; x_i and y_i are the measured and modelled velocity at the velocity survey point "i", respectively; $\bar{x}$ and $\bar{y}$ are the average measured and modelled velocity, respectively; n is the total number of velocity survey points; MAE is the mean absolute error.

Table 2 shows little statistical difference among case "E0.1", "E0.5" and "E10" in terms of the MAE, which indicates that the model results are not sensitive to background horizontal eddy viscosity. In order to pursue a higher correlation between the measured and modelled data, optimal background horizontal eddy viscosity was set as 0.1 m^2/s. The case "M0.035" has signification lower errors compared to case "M0.03", while higher correlation R compared to the case "M0.04". Thus, the optimal Manning roughness was set as 0.035. There is little statistical difference among case "G1.1", "G3.4" and "G6.5" in terms of correlation R and MAE, which means that a model with an average grid size of 6.5 m is sufficient to reproduce the real flow behaviours. Thus, the average grid size of 6.5 m, Manning roughness of 0.035, and background horizontal eddy viscosity of 0.1 m^2/s were determined as the calibrated parameters.

Figure 4 shows the comparison between the measured and modelled velocity as well as the differences at each velocimetry survey point when using the calibrated parameters. Relatively large errors can be seen in the first five cross-sections after the 14th St., which is probably because the model is unable to consider the impacts of the 14th St. bridge piers to the flow field immediately downstream. Overall, the modelled velocity matched with the measured velocity within a reasonable range, with a good correlation and a relatively low MAE. Thus, the calibration process is considered to be successful.

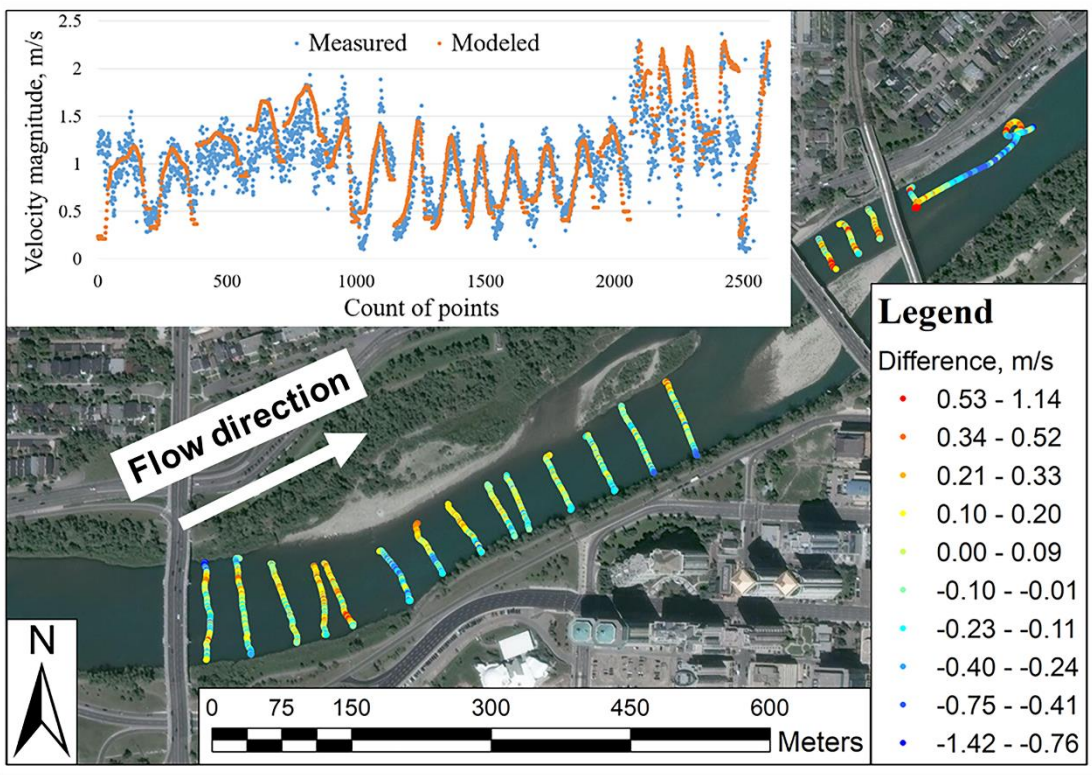

Figure 4. Comparison between the measured and modelled velocity as well as the differences at each velocimetry survey point when using the calibrated parameters. The imbedded plot shows the direct comparison between the modelled (yellow dots) and measured (blue dots) velocity: Points are sequenced from upstream to downstream, from left bank to right bank. The color map shows the velocity difference between the measured and modelled velocity: "Difference = modelled velocity – measured velocity".

2.3 Morphodynamic model

The morphodynamic model allows for the simulation of bed elevation updating and sediment transport. Most settings were directly adopted from the hydrodynamic model. Here only the differences are elucidated:

- **Bathymetry.** Since there were no high flows in year 2011 and 2012 that would cause significant sediment transport, the survey data on Sep 9, 2010 were used as the initial pre-flood bathymetry input for the morphodynamic model;
- **Roughness.** Manning roughness at vegetated places (i.e. bar surface, Prince's Island) was modified based on the suggested values in Phillips & Tadayon (2006). Places having bank protection structures were considered as none-erodible surfaces.
- **Bed stratigraphy.** Bed armouring was modelled by means of the bed stratigraphy module in Delft3D-FLOW, which consists two bed layers: the surface layer and the bookkeeping layer. Only sediments in the surface layer can directly interact with the flow. Once the surface layer is eroded, it gets replenished by the sediments from the bookkeeping layer below. Redundant sediments in the surface layer are pushed down to the bookkeeping layer if sediment deposits at the surface layer (Deltares, 2020). As such, the thickness of the surface layer is kept constant while the thickness of bookkeeping layer changes accordingly.
- **Sediment transport.** The thickness and sediment composition in each bed layer are shown in Table 3, which was based on the 1986 and 2016 bed surveys (see Table 1). Gauged data showed that sediments were mainly transported in the form of bedload in the model domain (Water Survey of Canada, 2013), which makes bedload the key control on the river morphology (Leopold, 1992; Williams et al., 2016). Thus, the suspended loads were not modelled. During the bedload transport process, small grains could be hidden from a current by larger, more exposed grains, known as the hiding-exposure effect. This effect is taken into account in this study by modifying the effective critical shear stress for different grain classes, using the formulation proposed by Parker et al. (1983). Bedload transport is also affected by bed level gradients. This effect is considered using the formulation proposed by Koch & Flokstra (1980). Different bedload transport formulas were trialed in the model validation stage, which will be covered in the next section.

Table 3.

Sediment composition in each bed stratigraphy layer

Layer	Initial thickness (m)	Sediment fractions	Median diameter (mm)	Mass fraction in the layer
Surface layer	0.3[#1]	No. 1	22.6	33%
		No. 2	89.4	33%
		No. 3	172.9	34%
Bookkeeping layer	4.0	No. 4	1.2	33%
		No. 5	30.9	33%
		No. 6	101.3	34%

- **Boundary conditions.** The hydrograph of the 2013 flood (See Figure 5) was used as the boundary conditions of the morphodynamic model. Due to the lack of measured bedload transport data at model boundaries during the flood, Neumann

boundary condition (i.e. sediment concentration gradient perpendicular to an open boundary equals to zero) was applied at the model boundaries to calculate the input/output bedload transport rate. This means that the bedload entering or leaving the model boundaries will be near-perfectly adapted to the local flow conditions (Deltares, 2020), which is mostly the case in the Bow River based on the historical gauged data (Water Survey of Canada, 2013).

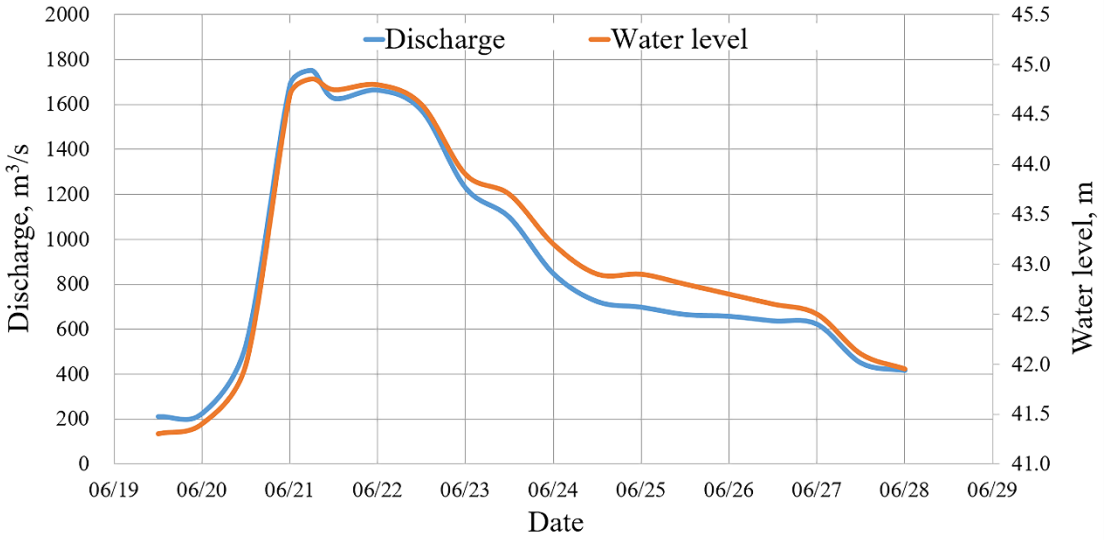

Figure 5. Hydrograph of the Calgary 2013 flood. Data were collected at the river gauge station 05BH004 (Water Survey of Canada, 2013)

2.4 Validation & sensitivity analysis

In this section, the influences of different sediment transport formulas, model dimension, and the location of the inflow boundary to the model performance were assessed by running several model scenarios. Results of those scenarios were evaluated by comparing the modelled and measured post-flood bed elevation in terms of MAE (Table 4).

Table 4.

Model validation and sensitivity analysis scenarios and corresponding statistical results.

Case	Setups			Statistical results	
	Sediment transport formula	Model dimension	Inflow boundary location	Overall MAE, m	MAE at bars, m
Case 1	Van Rijn (1993)	2D	Broadview Park	0.688	0.593
Case 2	Van Rijn (1993)	2D	14 St. SW Bridge	0.692	0.371
Case 3	Van Rijn (1993)	3D[#1]	14 St. SW Bridge	1.483	0.734
Case 4	Soulsby/Van Rijn (1997)	2D	14 St. SW Bridge	0.607	0.446
Case 5	Meyer-Peter-Muller (1948)	2D	14 St. SW Bridge	0.643	0.478

[#1] the developed 3D model has 4 flow layers and uses k-Epsilon model for 3D turbulence closure

Three bedload transport formulas were trialed: Van Rijn (1993), Soulsby/Van Rijn (1997), and Meyer-Peter-Muller (1948) (case 2, 4, & 5 in Table 4). It could be seen that Van Rijn (1993) produced the closest prediction in terms of the bar formation while Soulsby/Van Rijn (1997) produced the closest overall prediction. Since bar management and accurate prediction of subsequent bar formation are the major concerns in this study, Van Rijn (1993) was used in the following modelling works.

There was some concern that the upstream boundary (at 14 St. SW Bridge) is very close to the Poppy Plaza bars as well as the 10th St. bars (See Figure 1c). This proximity might result in inaccurate sediment transport predictions at those bars, with the implementation of Neumann boundary condition. Thus, the model sensitivity to the upstream boundary location was analyzed by moving the original upstream boundary 900 m further upstream to the Broadview Park (See Figure 1c) and compared the results (case 1 & 2 in Table 4). The model sensitivity to the model dimension was also analyzed by changing the dimension from 2D to 3D and comparing the results (case 2 & 3 in Table 4). It could be seen that changing the upstream boundary location or the model dimension didn't bring better results. Thus, the original upstream boundary and a model dimension of 2D were adopted in the following modelling works.

Figure 6 shows the measured pre-flood bed elevation, measured post-flood bed elevation, modelled post-flood bed elevation using the validated settings, and the difference between the modelled and measured post-flood bed elevation. It can be seen that the model overestimated the post-flood bed elevation at the ice anchor site (dashed circle in Figure 6a) and near the outer bend. The model also overestimated the volume of the 10th St. bar. Nonetheless, the developed model successfully reproduced the bar growth during the 2013 flood with respect to both location and height. The overall bed form produced by the model was also similar to the measured one, especially around the 10th St. bar and Poppy Plaza bars. From our perspective, the developed model was considered to be valid and ready for the simulations of bar management plans. However, the overestimation of deposition needs to be considered when interpreting the simulation results.

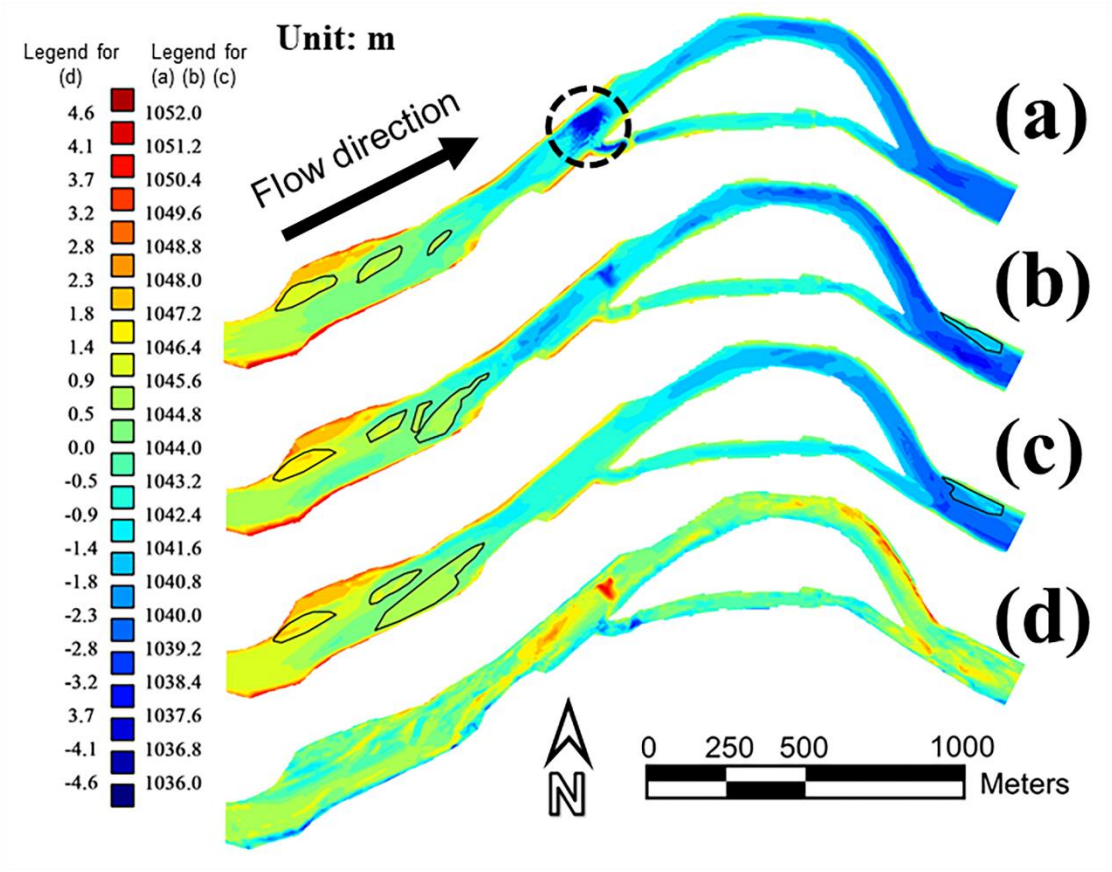

Figure 6. (a) Measured pre-flood bed elevation map (triangular interpolated from the ADCP survey points). Polygons mark the observed locations of channel bars. Dashed circle marks the ice anchor site; (b) Measured post-flood bed elevation map (triangular interpolated from the ADCP survey points). Polygons mark the observed locations of channel bars; (c) Modelled post-flood bed elevation map using the validated settings. Polygons mark the modelled locations of channel bars; (d) Difference between the measured and modelled maps (Difference = modelled value – measured value). Floodplains are excluded from the map for better illustration.

2.5 Bar management plans

Bar management was carried out for the 10th St. bar and the Poppy Plaza bars (see Figure 1c). The measured post-flood DEM was modified to reflect the implementation of different bar management plans. Those original vegetated and non-erodible places will be kept by using the same Manning roughness unless they are modified or removed in the proposed management plans. Three bar management plans (see Figure 7) were implemented and modelled in this study:

(1) "Do nothing". The river bars were not modified (Figure 7a). This plan was designed to avoid any possible negative consequences brought by human intervention. It is also a reference option to the other two bar management plans.

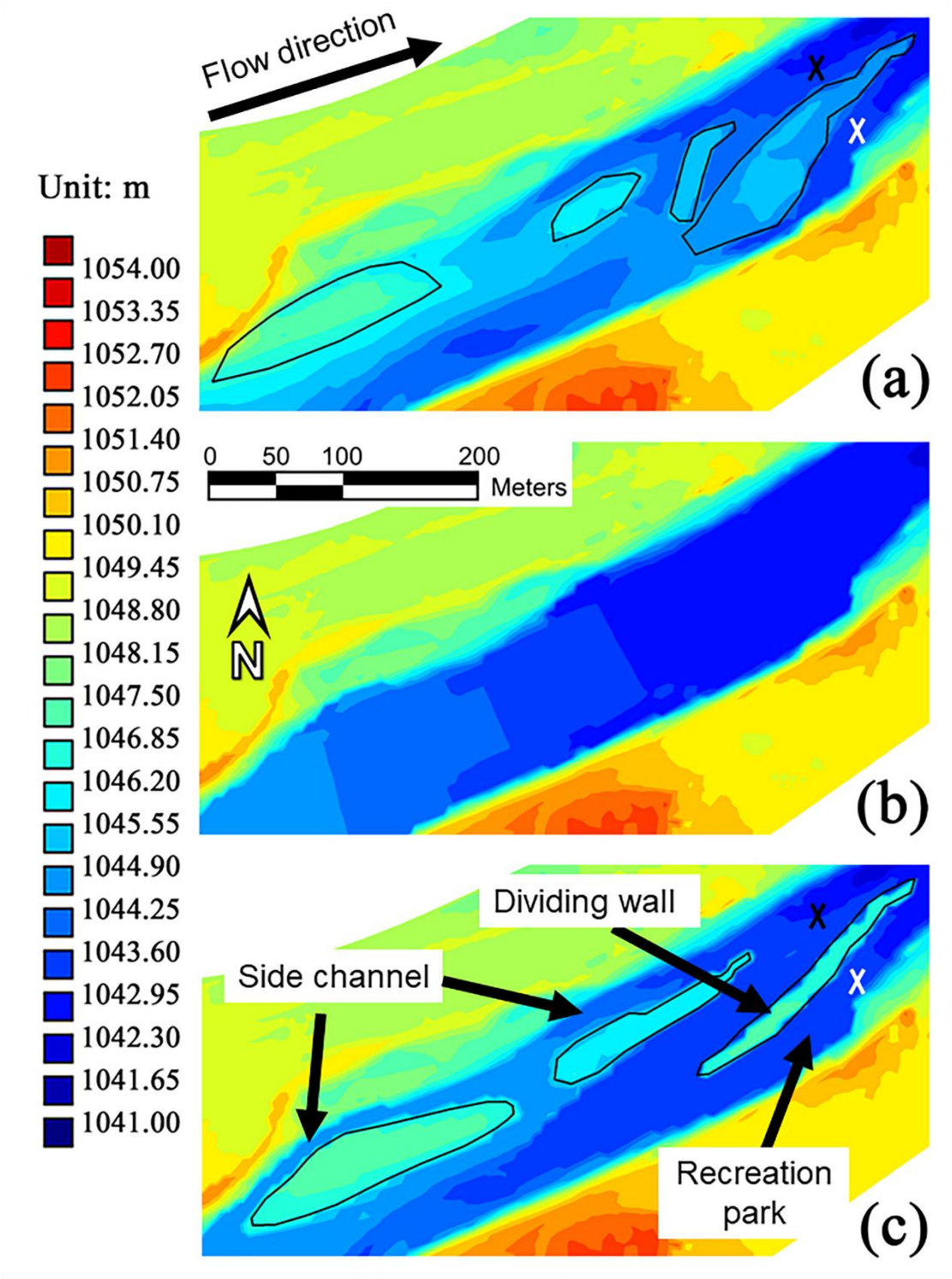

Figure 7. Bed elevation map of bar management plans: (a) no management; (b) bar removal; (c) bar realignment. Polygons mark the locations of channel bars. Black and white crosses mark the modelled velocity inspection sites during the long-term simulation (see Figure 12 for details). Black crosses: left side channel; white crosses: right side channel.

(2) "Bar removal". All gravel bars around the 10th St. Bridge as well as the Poppy Plaza were removed from the channel (Figure 7b) to lower the future flood peak to the largest extent. A constant stream-wise bed surface slope was assigned at the removal sites in order to smoothly connect the upstream and downstream edge of the removal sites.

(3) "Bar realignment". The bar realignment plan was designed (Figure 7c) in order to ① restore the active channel width, ② reduce flow blockage due to the bars, ③ create new aquatic habitat, ④ create a river recreation park for surfing and kayaking. In order to minimize the possible negative consequences brought by human intervention, the total instream sediment volume before and after the bar realignment action is maintained. First, 10th St. bars will be cleared. Some of the cleared volume will be piled up to construct a wall at the middle of the channel, functioning as a flow guider and a divider. The surface of the dividing wall will be covered with riprap to prevent erosion (i.e. non-erodible). The south side of the wall will be used to construct a recreation park. Then, a side channel will be excavated at the north side of the Poppy Plaza bars, functioning as a shallow channel for fish spawning habitat. Finally, the removed gravels were realigned to the top and the tail of the bars near the Poppy Plaza.

2.6 Design hydrographs

A future flood hydrograph is required for the morphodynamic model to simulate the performance of different bar management plans. In order to make the future hydrography closer to the reality, the hydrography was designed based on the historical daily instantaneous flow records from 1911 to 2021 (Water Survey of Canada, 2013). First, according to the study done by Slaney et al. (2019), significant bedload transport is expected to begin at around an 8-year flood ($Q \approx 700\ m^3/s$) for the Bow River. Thus, those floods with the peak discharge less than $700\ m^3/s$ were filtered out from the records. The remaining floods were two 10-year floods, one 25-year flood, one 35-year flood, and one 100-year flood. Then, the hydrograph of those floods was directly adopted and arranged together in 16 days (See Figure 8). Two 10-year floods were compacted in the first 4 days to represent an equivalent simulation of about 20 years, which will be noted as the "short-term" period hereafter. The entire hydrograph (i.e. 16 days) is equivalent to a simulation of about 100 years, which will be noted as the "long-term" period hereafter.

In Delft3D-FLOW, the morphological updating process could be accelerated by using the "morphological time scale factor", *MorFac*, in order to save the computational cost. *MorFac* has been used by a number studies to model the time-consuming long-term morphological process (e.g., Lesser et al., 2004; Moerman, 2011; Mool et al., 2017; Parsapour-Moghaddam et al., 2019b; Schuurman et al., 2013; Williams et al., 2016). *Morfac* is implemented in the sediment continuity equation of Delft3D-FLOW:

$$\Delta_{SED}^{(m,n)} = \frac{\Delta t \cdot f_{MorFac}}{A^{(m,n)}} \cdot \left[Q_u^{(m-1,n)} - Q_u^{(m,n)} + Q_v^{(m,n-1)} - Q_v^{(m,n)} \right] \quad (3)$$

where $\Delta_{SED}^{(m,n)}$ is the change in quantity of bottom sediment at computational cell (m,n) [kg/m^2]; Δt is the computational time step [s]; f_{MorFac} is the user-defined morphological time scale factor, *MorFac* [-]; $A^{(m,n)}$ is the area of cell (m,n) [m^2]; $Q_u^{(m,n)}$ is the computed bedload sediment transport rate in the u direction at cell (m,n) [kg/s].

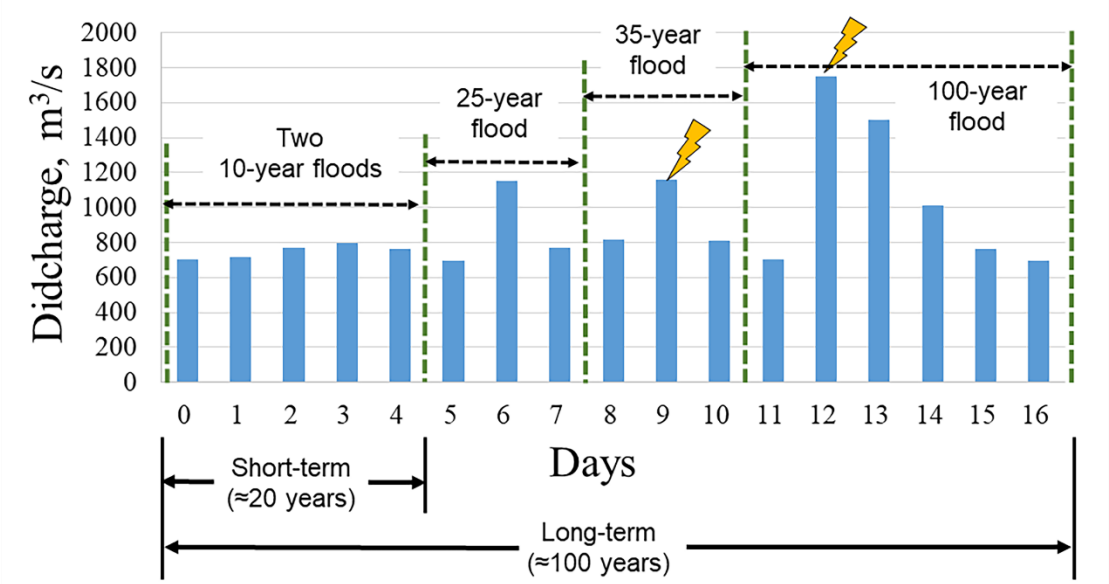

Figure 8. The designed future hydrograph. The lighting bolt symbols represent the flood peaks that are going to be investigated and compared between different bar managements in terms of flood mitigation.

The model sensitivity to *MorFac* needs to be analyzed prior to use, as recommended by Delft3D (Deltares, 2020). To do this, we designed three model scenarios with different combinations of *MorFac* and the simulated event time while keeping the total equivalent event time as well as the time step the same: ① *MorFac* = 1, simulated event time = 16 days, equivalent event time = $16 \times 1 = 16$ days; ② *MorFac* = 5, simulated event time = 3.2 days, equivalent event time = $3.2 \times 5 = 16$ days; ③ *MorFac* = 10, simulated event time = 1.6 days, equivalent event time = $1.6 \times 10 = 16$ days. We ran those three scenarios with the bar management plan of "do nothing". Results showed very little differences between case ① and case ② in terms of the developed bed morphology (See Figure Sup1a & Sup1b in the *Supporting Information*). In contract, no bed level change were found in case ③ (See Figure Sup1c), which indicates the large model instability when using *MorFac* = 10. Thus, *MorFac* = 5 was adopted in subsequent simulations.

3. Results

In all three bar management plans, the morphological evolution pattern of the short-term and long-term simulations was similar. In addition, a similar pattern of flood mitigation could be found between the 35-year flood and the 100-year flood for all bar management plans. Thus, only the results of long-term morphological evolution as well as the 100-year flood of different bar management plans are presented herein. The results of short-term morphological evolution as well as the 30-year flood peak level of different bar management plans can be found in the *Supporting Information* from Figure Sup2 & Sup3.

3.1 Morphological impacts

Figure 9 & 10 shows the cumulative deposition (or erosion) map and bed elevation map of different bar management plans after the long-term simulation, respectively. The simulation results show that:

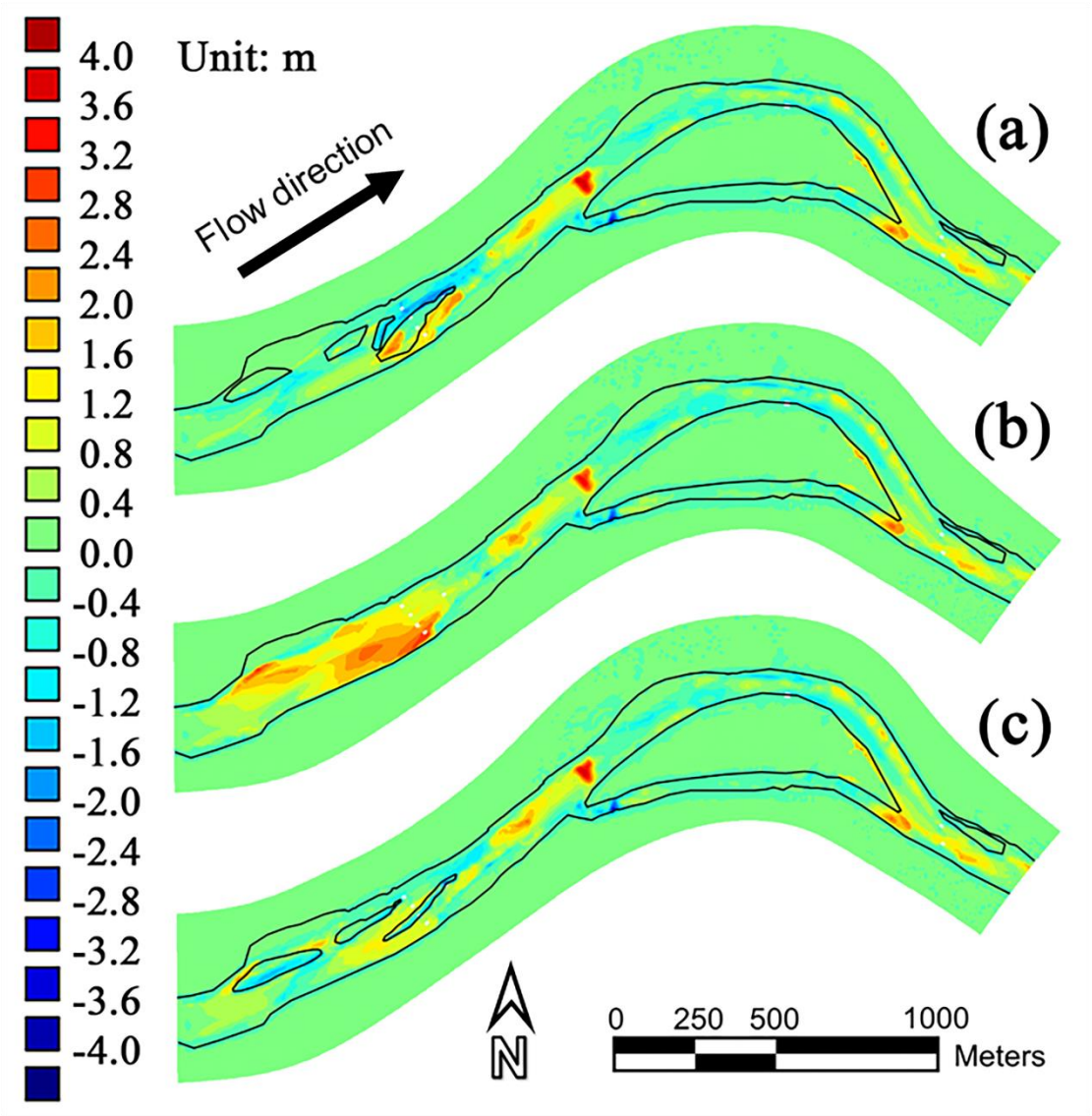

Figure 9. Cumulative deposition (red) and erosion (blue) map of different bar management plans after the long-term simulation: (a) Do nothing; (b) bar removal; (c) bar realignment. Polygons show the channel boundary and the channel bars before the run.

- **Do nothing.** If nothing is done on the instream bars, deposition will keep occurring at the tip and the right side of the 10th St. bar while erosion will happen at the left side of the 10th St. bar (Figure 9a) after the long-term simulation, which will result in a total occupancy of the right side of the river channel and a deep scour hole near the bridge piers (Figure 10a).

- **Bar removal.** As for the bar removal plan, abundant deposition happens at the bar removal sites. If comparing with the original bars, it can be seen that the new bars deposit at similar locations but with smaller dimension and lower height, compared to the original bars (Figure 7a and 10b). Different from the "do nothing" plan, the overall bed form will be nearly uniform and flat after the long-term simulation following bar removal.

- **Bar realignment.** In the bar realignment plan, minor deposition is predicted to happen around the tip of the dividing wall as well as at the entrance of the side channel near the Poppy Plaza bars (Figure 9c). The overall bed form at the bar management site does not change too much, compared with the other two

management plans. No deep scour hole or high-elevated bars are observed in the results of bar realignment.

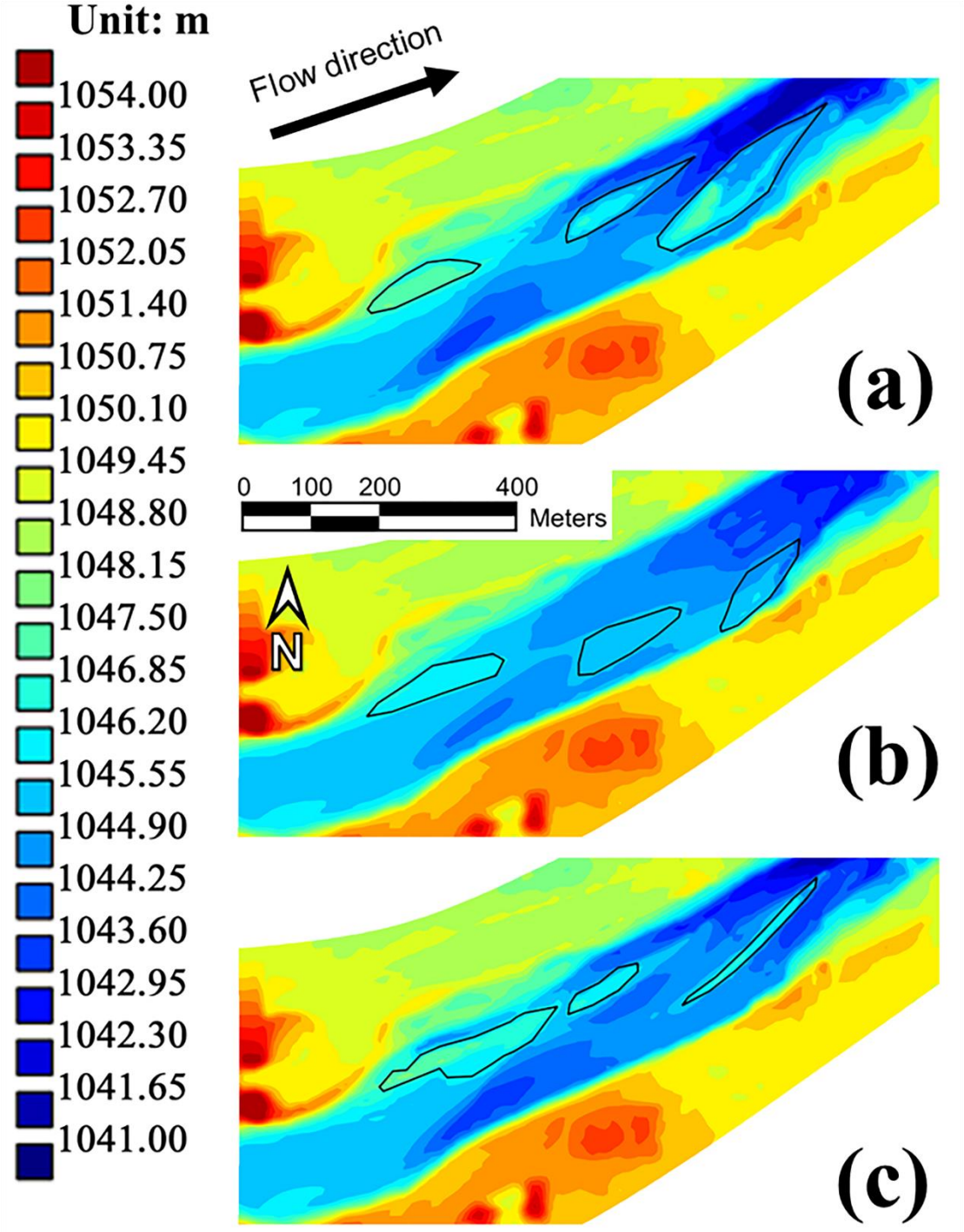

Figure 10. The bed elevation map of different bar management plans after the long-term simulation. (a) Do nothing; (b) bar removal; (c) bar realignment. Polygons show the channel bars after the run.

Noteworthy, similar downstream morphological impacts are predicted by the model regardless of the choice of bar management plans, which are: deposition is predicted to happen at the beginning and the end of the river bend while slight erosion will happen at the channel bed within the river bend. The long-term simulation results did not show any clear bank erosion for all three bar management plans.

3.2 100-year flood peak level

Figure 11 shows the flood mitigation performance of bar removal and bar realignment in terms of the modelled 100-year flood peak level. The mitigation performance was evaluated by calculating the 100-year flood peak level difference between the manipulation plans (i.e. bar realignment and bar removal) and the "do nothing" plan.

Bar removal is predicted to lower the 100-year flood peak by 0.26 m on average at the bar management site (dashed rectangle in Figure 11a). In contrast, bar realignment lowers the flood peak by 0.07 m on average at the bar management site (dashed rectangle in Figure 11b). Noteworthy, the flood peak level is predicted to be increased by about 0.15 m near the dividing wall in the bar realignment plan. No obvious flood level change is found for the downstream reaches in either case. In addition, by investigating the overbank flood extent, it can be seen that bar removal is predicted to result in a slightly smaller overbank flood extent compared to bar realignment (red arrows in Figure 11).

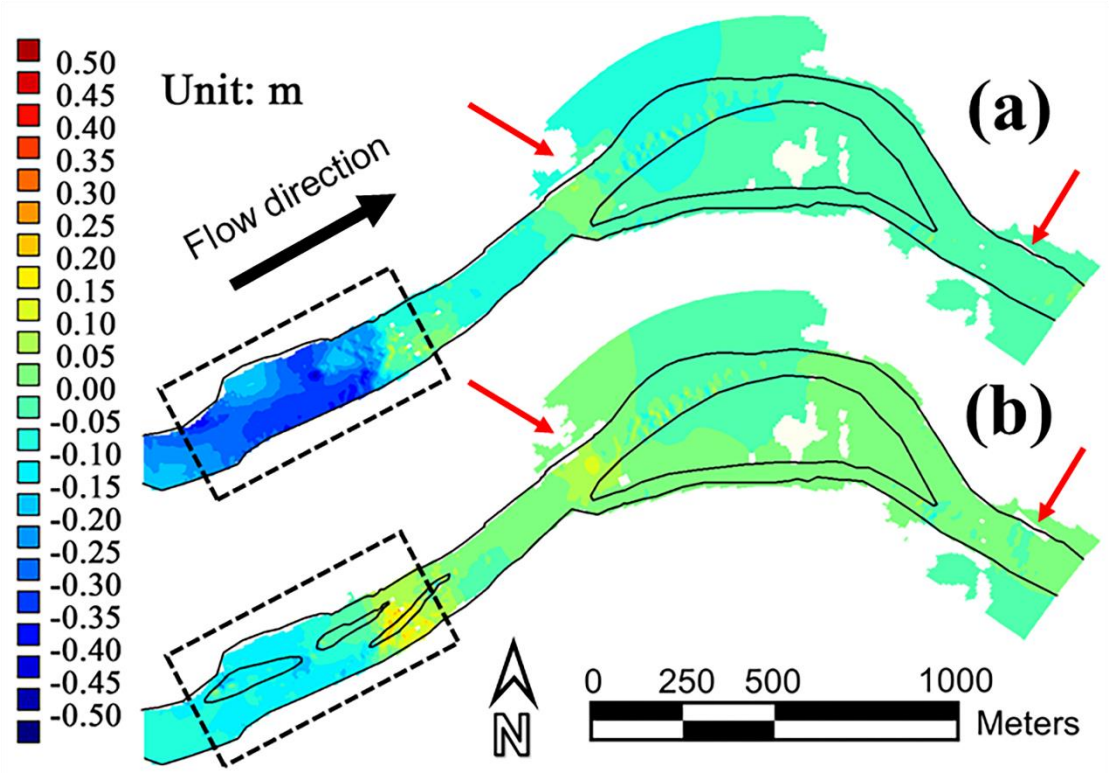

Figure 11. The 100-year flood peak level difference (a) between "bar removal" and "do nothing" (Difference = bar removal – do nothing), (b) between "bar realignment" and "do nothing" (Difference = bar realignment – do nothing). Red arrows show the locations of flood extent differences between bar removal and "do nothing". Dashed rectangles represent the "bar management site"

4. Discussion

4.1 Morphological impacts

If nothing is done to the instream bars around the 10th St. Bridge, deposition is predicted to happen at the tip of the 10th St. bar in the following flood events. The deposition site is right ahead of the site of dense vegetation at the 10th St. bar surface, which confirms that riparian vegetation colonization on the bar surface would induces additional resistance to the flow, thus cause sediment aggregation around the bar during the next flood event. Deposition is also observed in the right side channel (looking from

upstream) near the 10th St. bar, which is probably owing to the low flow velocity in the right side channel (the orange dashed line in Figure 12). Figure 10a shows the deposition at the right side channel would block the right side channel, which makes the floodwater mostly go through the left side channel. As a result, velocity in the left side channel dominates (the blue dashed line in Figure 12), which further causes significant scour at the left side channel (about 1.5 m deep, see Figure 9a). This scour would impact the stability of the bridge piers and also the left channel bank. In summary, the "do nothing" plan is predicted to result in a narrower and deeper river channel at the bar management site after a long-term period, compared to the original river channel.

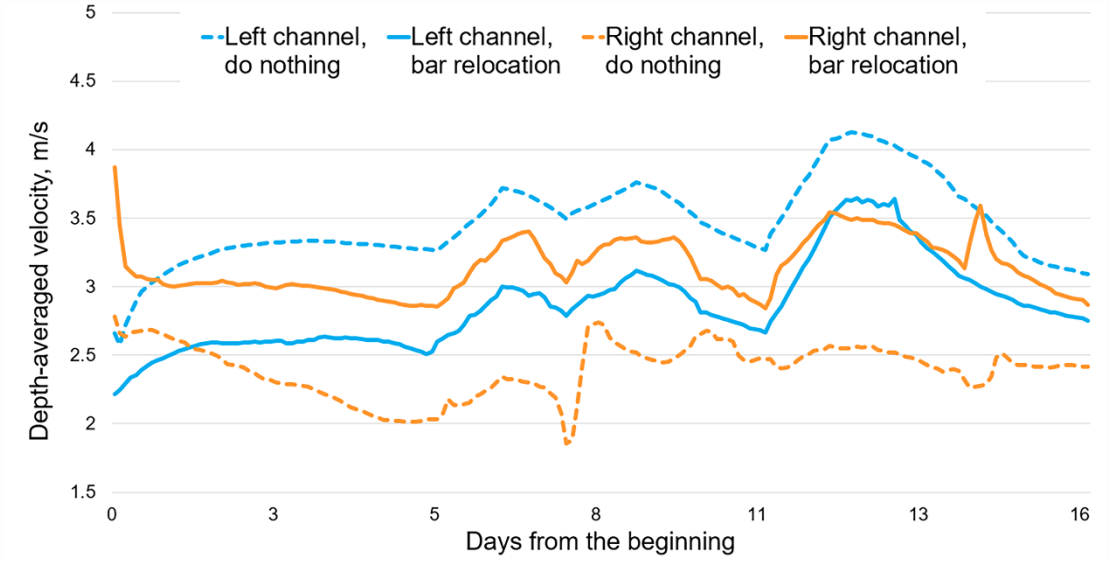

Figure 12. Time-series of modelled velocity at the right side channel (orange lines) and left side channel (blue lines) near the 10th St. bar/dividing wall for the "do nothing" plan (dashed lines) and bar relocation plan (solid lines) during the long-term simulation. Velocity inspection sites are marked by black (left side channel) and white crosses (right side channel) in Figure 7.

In the bar removal plan, bars are predicted to reoccur at the bar management site after several flood events. This is probably because the channel widens when flow enters the bar management site, which makes the flow velocity drop and thus causes deposition. The bar recurrence phenomenon has been widely observed both from field works (e.g. Church et al., 2001; Collins & Dunne, 1990; Yuill et al., 2016) and numerical studies (e.g. Li et al., 2008; Yuill et al., 2016; Parsapour-Moghaddam et al., 2019b), which reflects the resilience of alluvial river channels to an external disturbance. However, uncertainty remains in terms of the size of the reoccurred bars compared to the original bars: the reoccurred bar in Li et al. (2008) was lower in height compared to the original bar after a simulation of 10 years. In contrast, the reoccurred bars in Parsapour-Moghaddam et al. (2019b) were found to be bigger than the original bars. In this study, the reoccurred bars were both smaller and lower compared to the original bars before the bar removal after the long-term simulation, which coincides with the finding in Li et al. (2008) but different with Parsapour-Moghaddam et al. (2019b). This is probably because the *MorFac* used in Parsapour-Moghaddam et al. (2019b) was 20, which could result in significant model instability issues, as reported by Williams et al. (2016).

Similar to the plan of "do nothing", the dividing wall in the bar realignment plan also induces blockage to the flow, which results in deposition at the tip of the dividing wall. However, the deposition amount at the tip in the bar realignment plan is much smaller compared to that in the "do nothing" plan (Figure 9a & 9c). This is because the blockage effect of the thin dividing wall to the flow is smaller than the effect of a wide 10th St.

bar. After constructing the dividing wall, the channels on each side of the dividing wall have similar width and thus similar flow velocity (see Figure 12), which prevents significant erosion/deposition from happening at both side channels. Overall, the bar realignment plan is predicted to produce the most stable bed form at the bar management site after a long-term simulation compared with the other two plans.

In terms of downstream morphological impacts, both the bar realignment plan and the "do nothing" plan resulted in similar downstream bed morphology between the short-term (Figure Sup 2a & 2c) and long-term simulation (Figure 9a & 9c). This is because both of these two plans preserve the instream sediment volume, which brings little impact to the overall bedload transport pattern at the reach scale. Different from the bar realignment plan and the "do nothing" plan, very little deposition is found at the ice anchor site in the bar removal plan after the short-term simulation (Figure Sup 2b). This is because bar removal clears and widens the river channel and create a large area of "sediment-starving" regions at the beginning of the simulation. These regions capture most of the sediment coming from upstream and prevent them from going further downstream during the two 10-year floods. As the sediment accumulates in these regions, the "sediment-starving" situation is mitigated. Thus, after the two 10-year floods, much less subsequent deposition happens at the bar removal site, compared to the depostion during the two 10-year floods (i.e. not much difference at the bar removal site between Figure Sup 2b & Figure 9b). Excessive sediment is transported further downstream to the ice anchor site and deposits (Figure 9b). Excessive sediment is transported further downstream to the ice anchor site and deposits (Figure 9b). It could be seen that although bar removal may generate a short-term sediment deficit to the downstream reach, this deficit could be mitigated or even eliminated in a long-term period. As for the further downstream places (i.e. around Prince's Island and Center St. Bridge), the morphological evolution pattern is similar among all three management plans, both in short-term and long-term, which demonstrates the impact range of such intervention is very limited (about 1 km). In the end, the downstream morphological patterns of the three different bar management are predicted to be similar, which agrees with the filed work results in Wishart et al., (2008). Thus, it could be concluded that manipulation on vegetated bars has little morphological impacts to downstream reach.

4.2 Flood mitigation

Figure 11 indicates that the "do nothing" plan has the highest 100-year flood peak level at the bar management site among all three bar management plans, which confirms the hypothesis that the existing bars pose a high flood risk to the city. Figure 11 also shows that the bar removal plan results in a lower 100-year flood peak level at the bar management site and a slightly smaller downstream flood extent, compared to the bar realignment plan. Similar results could be found for the 30-year flood peak level (see Figure Sup3). Thus, based on the simulation results, the bar removal plan performs the best in terms of flood risk mitigation among the three bar management plans. However, the constructability and impacts of wholesale dredging in bar removal are significant and likely not practice in this case. As for the bar realignment plan, in order to preserve the volume of instream bars, some excessive sediment is piled up to form the dividing wall at the design stage. This high-elevated dividing wall is considered to increase the 100-year flood peak level near the dividing wall. Regardless, the designed bar realignment plan in this study does mitigate the flood risk at most places of the bar management site, which demonstrates the potential of generic bar realignment actions in terms of flood mitigation. In other words, if instream bars are realigned in a different

way, it is reasonable to believe that the new plan will result in an even better flood mitigation effect. In addition, some combination of the bar removal and realignment options might also present a good option in terms of flood mitigation.

There is an interesting phenomenon in the relation between flood peak mitigation and bed elevation change: bar removal is predicted to lower the 100-year flood peak by 0.26 m on average at the bar management site (Figure 11a), compared with the "do nothing" plan. However, the average bed elevation difference at the bar management site between bar removal and "do nothing" at the time of 100-year flood peak is only 0.0029 m (see Figure 13). This high inconsistency indicates that the quantitative bed elevation difference between those two cases at the time of 100-year flood peak is not the fundamental cause of the flood peak reduction. To the authors' point of view, this reduction is because the bar removal case brings a more uniform and less obstructed bed form compared to the "do nothing" case at the time of 100-year flood peak, which resulted in a lower flow resistance and thus greater ability to convey flood water. In comparison, the average bed elevation difference at the bar management site between bar realignment and "do nothing" at the time of 100-year flood peak is 0.07 m (Figure 11b). Since the sediment volume in the bar realignment case is preserved, the mitigation to the flood water blockage is limited. Thus, the quantitative bed elevation difference becomes dominant in the determination of the flood peak reduction, which is 0.07 m in average at the bar management site (Figure 13). It could be learned that simply relating the lowering of flood peak level to the lowering of river bed level could be misleading. Because the propagation of floodwater is a continuous and highly dynamic progress. Flood peak could still be lowered through altering the river bed form and lowering flow resistance, with or without lowering of river bed level. The approach of creating a uniform, less obstructed river bed form needs to be paid more attention in terms of fluvial flood mitigation.

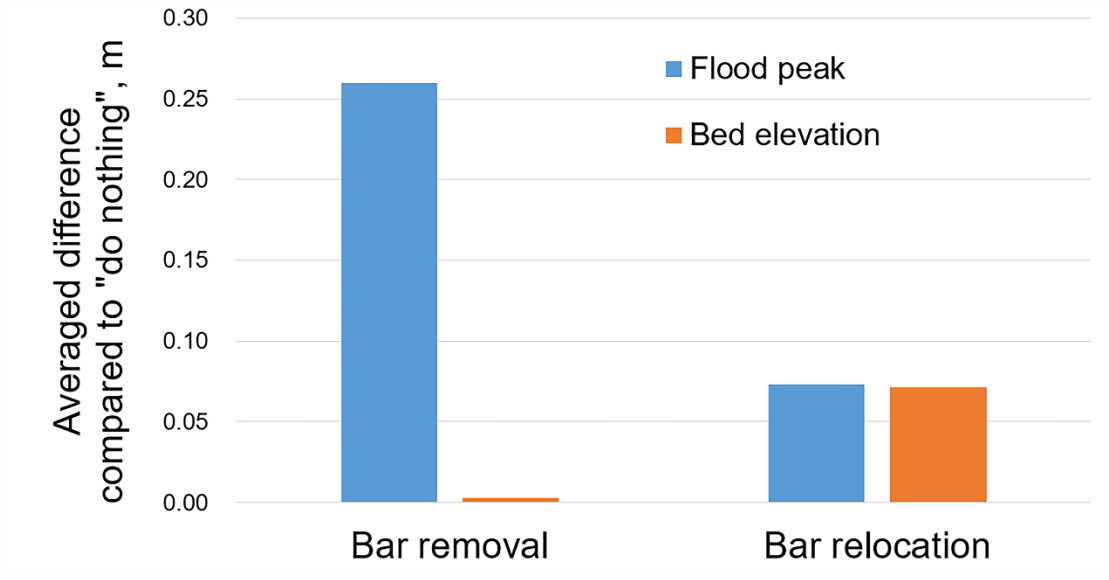

Figure 13. The average flood peak difference and bed elevation difference at the bar management site between bar removal (or bar realignment) and "do nothing" at the 100-year flood peak. Difference = "do nothing" - "bar removal" (or "bar realignment").

4.3 Aquatic habitat & river recreation

Figure Sup 2b shows that after total bar removal, it will likely require several bed mobilizing flood events and thus possibly decades for the bars to reform. During those

years, the bed morphology at the bar removal site will be relatively flat and uniform, which is generally unfavorable for fish habitat. Even after the recurrence of the instream bars, the overall bed morphology is still more uniform and lower in variety compared to the bar realignment plan or "do nothing" plan. In contrast, after the long-term run of using the bar realignment plan, although the entrance to the designed fish-spawning side channel near the Poppy Plaza bar is blocked, the side channel is still accessible during high-flow, which could provide refuge for fish during floods. In addition, the bed form variety in the bar realignment plan is quite high and remains relatively stable without significant deposition or erosion after a quite long term. This provides a favorable condition for aquatic ecosystem development for fish, water birds, as well as aquatic plants. In summary, the bar realignment plan performs better in terms of the protection of aquatic habitat compared to the bar removal plan.

At the design stage of different bar management plans, a river recreation park was proposed at the right side of the dividing wall in the bar realignment plan. According to the long-term simulation results (Figure 11c), no significant deposition or erosion occurs at the right side channel, which indicates that the river recreation park could maintain its normal functionality for a long time without maintenance works such as dredging. In contrast, this site was both filled with sedimentation in the bar removal plan and the "do nothing" plan. In conclusion, the bar realignment performs the best in terms of the realization of river recreation purpose among all three bar management plans.

4.4 Limitations and future concerns

The use of numerical models always involves a compromise between the computational cost and model details. In addition, numerical models also require a series of assumptions to represent and simplify the actual physical process and properties, which brings additional uncertainties to the results. Limitations of this study are addressed herein for further improvement:

- In order to save computational cost, the model domain only includes a part of the dry land, which prevents the floodwater to propagate further across the inland model boundary. Nonetheless, the modelled flood inundation areas match with the observed flood extent (Zhang & Crawford, 2020). Thus, this limitation was not considered to influence the model results, especially the morphodynamic aspect. Future study could extend the model domain so that the overall flood extent could also be used as a validation parameter.

- Impact from climate change is not considered in the design hydrograph, which limits the application of the projection results. Nonetheless, this study mainly focuses on the comparative study of the performance of different bar management plans. Thus, results are still meaningful to understand instream bar management and guide engineering practice. Climate change could be introduced in future studies to study the resulted bed form of a pre-selected bar management plan in a more accurate manner.

- Delft-3D is not capable of modelling the colonization process of bar surface vegetation during a series of flood events. In reality, the bar removal option might create new bars that quickly vegetate and become permanent, they may be even more stable, grow even faster, and result in even higher flood levels at the bar management site than the model assumes. Thus, the actual flood mitigation effect

of bar removal might not be that good. Again, since this study is mainly a comparative study and the colonization process is not considered for all three cases, results are still meaningful.

5. Conclusion

In this study, we developed a high-resolution morphodynamic model to reproduce the flood-induced morphological change in the Bow River, Calgary. We then utilized the developed morphodynamic model to evaluate the performance of three gravel bar management plans in terms of morphological impacts, flood mitigation, aquatic habitat protection, and possible river recreation use. This study demonstrates the consequences of instream bar management to the riverine environment and shows the great potential of a morphodynamic model as an impact and risk assessment tool. Several conclusions could be drawn herein:

- If no management action is taken to deal with the flood-induced instream bars in Bow River, the river channel is predicted to become narrower and deeper near those bars, which brings instability issues to the bridge piers and a high flood risk to the riverine neighborhood.

- Bar removal may bring a sediment deficit at the removal site, which induces bars recurrence. The reoccurred bars are predicted to be both smaller and lower compared to the original bars. Although bar removal presents the best flood mitigation effect among all three plans, the constructability and ecological impacts of wholesale dredging should not be overlooked.

- Bar realignment plan can stabilize the channel bed thus performs better in terms of aquatic habitat protection as well as the realization of river recreation. Although the proposed bar realignment plan in this study has limited ability to mitigate flood risk due to the construction of a dividing wall, it is reasonable to speculate that a different realignment strategy could have better mitigation effects.

- The downstream morphology could be affected in a short-term if the bar management plan brings sediment deficit to the river reach (i.e. bar removal). However, no matter which plan is applied, the downstream morphological patterns are predicted to be similar in a long-term. Thus, manipulation on vegetated instream gravel bars does not have obvious morphological impact to the downstream river reach.

- Simply relating the lowering of flood peak level to the lowering of river bed level could be misleading because the propagation of floodwater is a continuous and highly dynamic progress. Creating a uniform, less obstructed river bed is believed to be the fundamental strategy in flood mitigation.

Acknowledgements

The authors would like to thank The City of Calgary and the Natural Sciences and Engineering Research Council of Canada (grant CRDJP 524502-18) for funding this project. Many thanks to Xi Chen, for her assistance in image processing for official publication.

References

Brown, A.V., Lyttle, M.M., & Brown, K.B. (1998). Impacts of gravel mining on gravel

754 bed streams. *Transactions of the American Fisheries Society*. 127: 979-994.
755 https://doi.org/10.1577/1548-8659(1998)127<0979:IOGMOG>2.0.CO;2

756 Church, M. (1992) Channel morphology and typology. In: Calow P, Petts GE (eds) The
757 rivers handbook, vol 1. Blackwell, Oxford, pp 126–143

758 Church, M., Rempel, L., & Rice, S. (2000). Morphological and habitat classification of
759 the Lower Fraser River gravel-bed reach. Report prepared for the Fraser Basin
760 Council, November 2000: 77pp.

761 Church, M., Ham, D., & Weatherly, H. (2001). Gravel management in Lower Fraser
762 River. (Report). Department of Geography, University of British Columbia,
763 Vancouver, B.C., Canada. 110 pp

764 Collins, B.D. & Dunne, T. (1989). Gravel transport, gravel harvesting, and channel-bed
765 degradation in rivers draining the southern Olympic Mountains, Washington,
766 U.S.A. *Environmental Geology and Water Science*. 13: 213-224.
767 https://doi.org/10.1007/BF01665371

768 Collins, B. & Dunne, T. (1990). Fluvial geomorphology and river gravel mining: a
769 guide for planners, case studies included. California Department of Conservation,
770 Division of Mines and Geology, Special Publication 98: 29pp.

771 Deltares. (2020). "Delft3D-FLOW user manual: Simulation of multidimensional
772 hydrodynamic flows and transport phenomena, including sediments." Delft,
773 Netherlands.

774 Exner, F. M. (1925), U¨ ber die Wechselwirkung zwischen Wasser und Geschiebe in
775 Flu¨ssen (in German), Sitz. Acad. Wiss. Wien Math. Naturwiss. Abt. 2a, 134, 165-
776 203.

777 Golder Associates (2011). Bow and Elbow River updated hydraulic model project:
778 survey data collection and DEM data creation. Prepared for the City of Calgary.

779 Golder Associates (2015). Bow and Elbow River updated hydraulic model project:
780 survey data collection and digital elevation model creation. Prepared for the City
781 of Calgary.

782 Government of Alberta (2014). June 2013 Southern Alberta Floods, One Year Report.
783 Available at https://www.alberta.ca/AlbertaCode/images/Flood-Recovery-One-
784 Year-Report.pdf Accessed April 2, 2018

785 Kasvi, E., Alho, P., Lotsari, E., Wang, Y., Kukko, A., Hyyppä, H., & Hyyppä, J. (2015).
786 Two-dimensional and three-dimensional computational models in hydrodynamic
787 and morphodynamic reconstructions of a river bend: sensitivity and functionality.
788 Hydrological Processes, 29(6), 1604-1629. https://doi.org/10.1002/hyp.10277

789 Klohn Crippen Berger (2016). Calgary Rivers Morphology and Fish Habitat Study:
790 Geological Review of the Bow and Elbow Rivers. Prepared for the City of Calgary.

791 Koch, F. G. & Flokstra, C. (1980). Bed level computations for curved alluvial channels.
792 In Proceedings of the XIXth congress of the International Association for
793 Hydraulic Research, 2-7 Feb. 1981, New Delhi, India, vol. 2, pages 357–364.

794 Kondolf, G. M. (1994). Geomorphic and environmental effects of instream gravel

mining. *Landscape and Urban Planning*. 28:225–243. https://doi.org/10.1016/0169-2046(94)90010-8

Kondolf, G.M., (1997). Hungry water: effects of dams and gravel mining on river channels. *Environmental Management*. 21, 533–551. https://doi.org/10.1007/s002679900048

Kondolf, G.M., & Wolman, M.G. (1993). The sizes of salmonid spawning gravels. *Water Resources Research*. 29:2275–2285. https://doi.org/10.1029/93WR00402

Kori, E. & Mathada, H. (2012). An assessment of environmental impacts of sand and gravel mining in Nzhelele Valley, Limpopo Province, South Africa. Proceedings, 3rd International Proceedings of Chemical, Biological, and Environmental Engineering; 137–141.

Leopold, L. B. (1992), Sediment size that determines channel geometry. *Dynamics of Gravel-Bed Rivers*, edited by P. Billi et al., pp. 297–311, Wiley, Chichester, U. K.

Lesser, G. R., Roelvink, J. A., Van Kester, J. A. T. M., & Stelling, G. S. (2004). Development and validation of a three-dimensional morphological model. *Coastal Engineering*, 51(8), 883-915. https://doi.org/10.1016/j.coastaleng.2004.07.014

Li, S.S., Millar, R.G., & Islam, S. (2008). Modelling gravel transport and morphology for the Fraser River Gravel Reach, British Columbia. *Geomorphology*, Volume 95, Issues 3–4, 2008, Pages 206-222, ISSN 0169-555X, https://doi.org/10.1016/j.geomorph.2007.06.010.

Mat Salleh, M.Z. & Ariffin, J. (2013). Flow and Sediment Matrix in Mid-Channel Bar Formation. *International Journal of Scientific & Engineering Research*. 4. 1757-1764.

Meyer-Peter, E., & R. Müller, (1948). Formulas for bed load transport. In Proceedings of the 2nd Congress IAHR, Stockholm, vol. 2, pages 39–64.

Miller, A.C., King, R.H., Glover, J.E., & Army engineer waterways experiment station Vicksburg MS environmental lab. (1983) Design of a Gravel Bar Habitat for the Tombigbee River Near Columbus, Mississippi. Defense Technical Information Center. 64 pages.

Mool, P., Popescu, I., Giri, S., Omer, A., Sloff, K., Kitamura, Y., & Solomatine, D. (2017). Delft3D morphological modelling of sediment management in daily peaking run-of-the-river hydropower (PROR) reservoirs in Nepal. 85th Annual Meeting of International Commission on Large Dams. July 3-7, 2017. Prague, Czech Republic.

Moerman, E. (2011). Long-term morphological modelling of the mouth of the Columbia River. Doctoral dissertation, Delft University, Netherlands.

Northwest Hydraulic Consultants Ltd. (1986). River Regime Study - Bow and Elbow Rivers at Calgary, Alberta. Prepared for the City of Calgary.

Parker, G., Klingeman, P. C., & McLean, D. G. (1983). Bedload and size distribution in paved gravel-bed streams. *Journal of Hydraulic Engineering*, 109(5), 793-794. https://doi.org/10.1061/(ASCE)0733-9429(1983)109:5(793)

Parsapour-Moghaddam, P., Brennan, C. P., Rennie, C. D., Elvidge, C. K., & Cooke, S.

J. (2019a). Impacts of channel morphodynamics on fish habitat utilization. Environmental management, 64(3), 272-286. https://doi.org/10.1007/s00267-019-01197-0

Parsapour-Moghaddam, P., & Rennie, C. D. (2017). Hydrostatic versus nonhydrostatic hydrodynamic modelling of secondary flow in a tortuously meandering river: Application of Delft3D. River research and applications, 33(9), 1400-1410. https://doi.org/10.1002/rra.3214

Parsapour-Moghaddam, P., Rennie, C.D., Slaney, J. (2019b) Morphodynamic modelling to evaluate flood mitigation strategies, 38th IAHR World Congress, Panama City, Panama, Sep 1-6, 10.3850/38WC092019-1083

Pauley, G. B., Thomas, G. L., Marino, D. A., & Weigand, D. C. (1989). Evaluation of the effects of gravel bar scalping on juvenile salmonids in the Puyallup River drainage. University of Washington Cooperative Fishery Research Unit Report. University of Washington, Seattle.

Petit, F., Poinsart, D., & Bravard, J.-P. (1996). Channel incision, gravel mining and bedload transport in the Rhone River upstream of Lyon, France ("canal de Miribel"). *Catena*. 26: 209-226. https://doi.org/10.1016/0341-8162(95)00047-X

Phillips, J. V. & Tadayon, S. (2006) Selection of Manning's Roughness Coefficient for Natural and Constructed Vegetated and Non-Vegetated Channels, and Vegetation Maintenance Plan Guidelines for Vegetated Channels in Central Arizona. Scientific Investigations Report. 2006-5108. https://doi.org/10.3133/sir20065108

Pomeroy, J.W., Stewart, R.E., & Whitfield, P.H., (2016). The 2013 flood event in the South Saskatchewan and Elk River basins: Causes, assessment and damages. *Canadian Water Resources Journal*. 41, 105–117. https://doi.org/10.1080/07011784.2015.1089190.

Rempel, L.L., Healey, K., & Lewis, F.J.A. (2012). Lower Fraser River juvenile fish habitat suitability criteria. Canadian Technical Report of Fisheries and Aquatic Sciences. 2991: ix + 73 p.

Rennie, C. D., & Church, M. (2010). Mapping spatial distributions and uncertainty of water and sediment flux in a large gravel bed river reach using an acoustic Doppler current profiler. *Journal of Geophysical Research: Earth Surface*, 115, F03035, https://doi.org/10.1029/2009JF001556

Rood, S.B., Kaluthota, S., Philipsen, L.J., Slaney, J., Jones, E., Chasmer, L., & Hopkinson, C. (2019) Camo-maps: An efficient method to assess and project riparian vegetation colonization after a major river flood. *Ecological Engineering*, Volume 141, 2019, 105610, ISSN 0925-8574, https://doi.org/10.1016/j.ecoleng.2019.105610.

Schuurman, F., Marra, W. A., & Kleinhans, M. G. (2013). Physics-based modeling of large braided sand-bed rivers: Bar pattern formation, dynamics, and sensitivity. *Journal of Geophysical Research: Earth Surface*, 118(4), 2509-2527. https://doi.org/10.1002/2013JF002896

Sear, D.A., & Archer, D. (1998). Effects of gravel extraction on stability of gravel-bed rivers: The Wooler Water, Northumberland, UK. In: Klingeman, P.C., Beschta, R.L., Komar, P.D., Bradley, J.B. (Eds.), Gravel-bed Rivers in the Environment.

Water Resources Publication, Highlands Ranch, CO, pp. 415–432.

Slaney, J., Rood, S., Dick, W., & Rennie, C. (2019). The city of Calgary's river morphology risk mitigation program. Proceedings of the 38th IAHR World Congress, Panama. 4202-4210. https://doi.org/10.3850/38WC092019-1423

Soulsby, R. (1997). Dynamics of marine sands, a manual for practical applications. Thomas Telford, London, United Kingdom.

Surf Anywhere. (2020). Initial design report for the Calgary River Wave Park at Calgary, Alberta. SA-2018-009-R1. Prepared for the City of Calgary. Access through: https://albertariversurfing.com/surfyyc

Surian, N. (1999). Channel changes due to river regulation: the case of the Piave River, Italy. *Earth Surface Processes and Landforms*. 24: 1135-1151. https://doi.org/10.1002/(SICI)1096-9837(199911)24:12<1135::AID-ESP40>3.0.CO;2-F

Veiga, V.B., Hassan, Q.K., & He, J. (2015) Development of Flow Forecasting Models in the Bow River at Calgary, Alberta, Canada. *Water*, 7, 99-115. https://doi.org/10.3390/w7010099

Van Rijn, L. C. (1993). Principles of Sediment Transport in Rivers, Estuaries and Coastal Seas. Aqua Publications, The Netherlands.

Water Survey of Canada. (2013) Real-Time Hydrometric Data. Access through: https://wateroffice.ec.gc.ca/search/real_time_e.html

Williams, R. D., Measures, R., Hicks, D. M., & Brasington, J. (2016). Assessment of a numerical model to reproduce event‐scale erosion and deposition distributions in a braided river. Water Resources Research, 52(8), 6621-6642. https://doi.org/10.1002/2015WR018491

Wintenberger, C.L., Rodrigues, S., Claude, N., Jugé, P., Bréhéret, J., & Villar, M. (2015). Dynamics of nonmigrating mid-channel bar and superimposed dunes in a sandy-gravelly river (Loire River, France), *Geomorphology*, Volume 248, Pages 185-204, ISSN 0169-555X, https://doi.org/10.1016/j.geomorph.2015.07.032.

Wishart, D., Warburton, J., & Bracken, L. (2008). Gravel extraction and planform change in a wandering gravel-bed river: The River Wear, Northern England. *Geomorphology.*, 94 (1-2). pp. 131-152. http://dx.doi.org/10.1016/j.geomorph.2007.05.003

Yuill, B. T., Gaweesh, A., Allison, M. A., & Meselhe, E. A. (2016) Morphodynamic evolution of a lower Mississippi River channel bar after sand mining. *Earth Surface Processes and Landforms*, 41: 526– 542. https://doi.org/10.1002/esp.3846.

Zeng, Q., Shi, L., Wen, L., Chen, J., Duo, H., & Lei, G. (2015) Gravel Bars Can Be Critical for Biodiversity Conservation: A Case Study on Scaly-Sided Merganser in South China. *PLoS One*. 10(5): e0127387. https://doi.org/10.1371/journal.pone.0127387

Zhang, Y., & Crawford, P. (2020). Automated Extraction of Visible Floodwater in Dense Urban Areas from RGB Aerial Photos. *Remote Sensing*. 12(14):2198. https://doi.org/10.3390/rs12142198